

Prototype high resolution multienergy soft x-ray array for NSTX^{a)}

K. Tritz,^{1,b)} D. Stutman,¹ L. Delgado-Aparicio,² M. Finkenthal,¹ R. Kaita,²
and L. Roquemore²

¹*Department of Physics and Astronomy, Johns Hopkins University, Baltimore, Maryland 21218, USA*

²*Princeton Plasma Physics Laboratory, Princeton, New Jersey 08543, USA*

(Presented 20 May 2010; received 15 May 2010; accepted 28 May 2010;
published online 4 October 2010)

A novel diagnostic design seeks to enhance the capability of multienergy soft x-ray (SXR) detection by using an image intensifier to amplify the signals from a larger set of filtered x-ray profiles. The increased number of profiles and simplified detection system provides a compact diagnostic device for measuring T_e in addition to contributions from density and impurities. A single-energy prototype system has been implemented on NSTX, comprised of a filtered x-ray pinhole camera, which converts the x-rays to visible light using a CsI:Tl phosphor. SXR profiles have been measured in high performance plasmas at frame rates of up to 10 kHz, and comparisons to the toroidally displaced tangential multi-energy SXR have been made. © 2010 American Institute of Physics.

[doi:10.1063/1.3460632]

I. MOTIVATION

Our previous work has demonstrated the utility of using “multienergy” soft x-ray (ME-SXR) profiles to infer changes in the electron temperature profile on fast (<1 ms) time scales.¹ This technique relies on the use of multiple pinholes with different filters viewing the same volume of plasma, which results in a coarse “subsampling” of the x-ray emission spectrum, which can then be used to extract information on the electron temperature, density, and potential impurity content by comparing the filtered emissivity profiles. However, the previous system had limitations, which reduced the accuracy of the temperature reconstruction in typical NSTX plasmas. The three pinholes and filters used were insufficient to constrain the reconstruction of plasmas with a significant amount of impurities, the lossy fiber optic coupling between the CsI:Tl phosphor, and the low quantum efficiency photomultiplier tube (PMT) amplifiers reduced the overall signal-to-noise ratio (SNR) of the system, and the radiation induced scintillation in the fibers further added to the noise of the measurements. A new ME-SXR design will overcome these difficulties by placing an image intensifier stage directly after the CsI:Tl phosphor output and using two-dimensional camera-based imaging to expand the number of filtered x-ray profiles to five to six. This paper will describe a prototype, single-energy system that was implemented on NSTX to test this measurement technique.

II. PROTOTYPE HARDWARE

The physical design of the prototype system (Fig. 1) uses a tangentially viewing pinhole camera configuration with an input slit 0.75 mm wide and 6.35 mm high. The slit is covered by a light-tight x-ray filter assembly, which uses a vacuum linear feed-through to select between a 10 μm Be foil, with a 1% transmission cut-off at an x-ray photon energy of ~ 600 eV and a 0.3 μm Ti foil, which has a similar high-energy x-ray transmission curve in addition to a transmission “window” at lower x-ray energies, between ~ 150 and 450 eV, admitting primarily carbon line radiation from the plasma edge.

The resultant tangential x-ray profile emission from the plasma is converted into visible light using a phosphor deposited on a fiber optic plate (FOP). Columnar CsI:Tl, deposited by RMD, Inc., was chosen because of its good time response (≤ 10 μs) and conversion efficiency (~ 25 γ/keV into 2π sr).² The output from the FOP is then directly coupled to the photocathode of a 25 mm diameter encapsulated microchannel plate (MCP) image intensifier mounted in a Conflat vacuum flange. At the maximum recommended voltages, the image intensifier can apply a gain of up to 10^4 e^-/e^- corresponding to a spectral amplification of ~ 5000 W/W at 550 nm with an S20 input photocathode and P20 output phosphor. This amplified image is then lens-coupled through a 3 m length coherent fiber optic imaging bundle to a Phantom v4.2 fast framing complementary metal-oxide semiconductor (CMOS) camera,³ capable of frame rates up to 14 kHz at a subsampled resolution of 256×128 pixels with a resolution of 8 bits per pixel. The output brightness of the image intensifier limited practical acquisition rates to <10 kHz, with a typical frame rate of 2 kHz providing a reasonable tradeoff between time resolution and SNR. The diagnostic used a tangential field-of-view (FOV) of the plasma at the midplane covering from the magnetic axis to the plasma edge.

^{a)} Contributed paper, published as part of the Proceedings of the 18th Topical Conference on High-Temperature Plasma Diagnostics, Wildwood, New Jersey, May 2010.

^{b)} Author to whom correspondence should be addressed. Electronic mail: ktritz@pppl.gov.

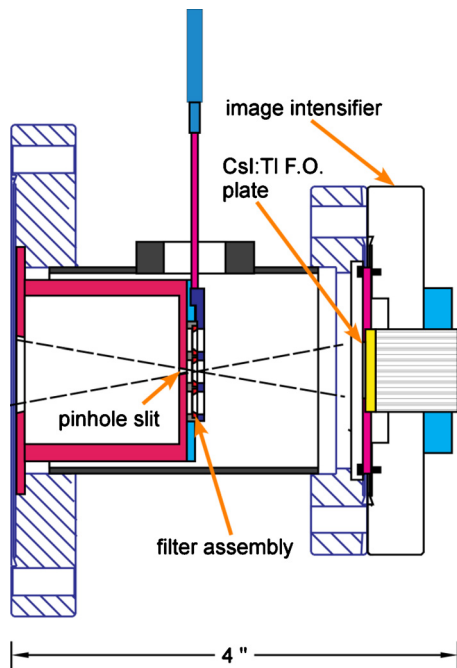


FIG. 1. (Color online) Schematic of the prototype ME-SXR diagnostic.

III. MEASUREMENT TECHNIQUE

A single frame from the camera imaging of the amplified soft x-ray signal is shown in Fig. 2. The acquired image is rotated 11.56° to obtain a horizontal measurement and then vertically integrated across the full width at half maximum of the image band to obtain a linear SXR intensity profile at the plasma midplane from the core to the edge. The radial profile from each camera frame is then assembled to provide a time history of the soft x-ray intensity over the entire plasma shot. The vertical signal integration uses ~ 40 pixels for a SNR improvement of $\times 6$ while maintaining the same radial spatial resolution. Each $22\ \mu\text{m}$ pixel of the CMOS detector maps to a $125\ \mu\text{m}$ square region on the CsI:Tl phosphor imager, which, when combined with the $750\ \mu\text{m}$ wide pinhole aperture, results in an effective $\sim 1.5\ \text{cm}$ radial spatial resolution in the plasma with $6\times$ spatial oversampling. Though the effective spatial resolution is set by the larger width of the slit aperture, the spatial oversampling does

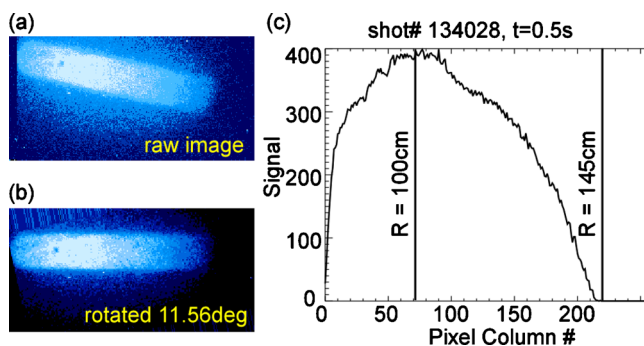


FIG. 2. (Color online) (a) The raw image from the Phantom v4.2 CMOS fast framing camera. (b) The image rotated to allow vertical integration. (c) The SXR intensity profile obtained by integrating each camera frame

improve the measurement of SXR profile and permits the detection of subcentimeter features. Due to port sharing and limitations on machine access, a postrun diagnostic calibration was impossible, though a geometric spatial calibration is consistent with the measurements and shows a smooth profile from the edge ($R_{\text{tan}} \sim 145\ \text{cm}$) to the center of the plasma ($R_{\text{tan}} \sim 100\ \text{cm}$) before vignetting from port structures begins to attenuate the signal for $R_{\text{tan}} < 100\ \text{cm}$.

The combination of dark noise and readout noise for the entire system is seven counts, with typical signals ranging from 10 s of counts at the plasma edge to ~ 800 counts in the core of high performance plasmas at frame rates of 2 kHz. The total noise of the system at peak plasma signals is ~ 9 –11 counts. Therefore, the system noise and photon noise (including excess noise from the MCP gain) are comparable at ~ 7 counts each. Slower frame rates exhibited the expected increase in SNR, with core signal levels of 4–5000 and the combination of dark and readout noise level at ~ 3 counts for a 300 Hz readout rate. With such low levels of inherent system noise, the photon noise is the dominant factor throughout the majority of the plasma discharge, and indeed the total noise during the peak plasma emission is ~ 20 –25 counts, though some of this variation may be attributed to the difficulty in finding a long enough period of plasma quiescence to statistically assess the true photon noise of the system. In comparison to the previous multienergy SXR system based on PMT amplifiers, the prototype image intensifier SXR system obtains $\frac{1}{2}$ the SNR with a much smaller étendue and 3 – $4\times$ improved spatial resolution. Comparing the two systems directly with the same spatial resolution, the prototype has $2\times$ better SNR, and further optimization of the optical train and coupling between the intensifier and CMOS camera could boost performance by another factor of 4 – 5 for a total improvement of $\times 10$ over the previous system. The prototype detector is also relatively immune to noise from neutrons and other high-energy radiation. Noise spikes from radiation can contaminate a few pixels on the CMOS detector image intermittently throughout the discharge, but these are easily detected and removed by comparing pixels on a frame-by-frame basis and interpolating over large outliers.

Though the NSTX plasma shot lasts on the order of a second, with ~ 10 min between discharges, the plasma shot length is long compared to the recharge time of the MCP channels ($\sim 10^{-2}\ \text{s}$).⁴ Therefore, the image intensifier is acting as a dc gain system rather than its typical application as a charged particle pulse height detector. Operation in the dc mode puts a strong constraint on the amount of charge that can be extracted from the MCP detector before the channels become depleted of charge and exhibit reduced nonlinear gain. In fact, this depletion becomes quite evident once the MCP channel exceeds $\sim 10\%$ of the maximum current and results in a gradual, nonlinear reduction of the channel gain with an eventual $10\times$ reduction of the peak signals of the SXR intensity profile compared to the PMT-based multienergy SXR system, which has a constant gain and linear signal response. Because the nonlinear charge depletion affects the photon signal and photon noise equally, it has no effect

on the overall SNR of the measurement, though it does make a quantitative assessment of the SXR profile problematic unless one can remain in the linear gain regime. However, one positive side effect of the channel charge depletion is an effective *increase* of the dynamic range of the system by effectively reducing the gain for the higher intensity of the SXR emission in the core relative to the edge pixels. Thus, the high sensitivity of the system is preserved in the low intensity pixels, allowing the detection of activity in the lower-signal edge region while still retaining some sensitivity in the charge-depleted, reduced MCP gain regime for the pixels that view the high SXR intensity plasma core.

IV. RESULTS

The prototype diagnostic operated successfully for several weeks during the previous 2009 NSTX run, taking measurements in standard high performance H-mode plasmas with central $T_{e0} \sim 1$ keV and electron density, $n_{e0} \sim 3\text{--}8 \times 10^{13} \text{ cm}^{-3}$. With its particular viewing geometry, the prototype system FOV intersects the neutral beams as they enter the plasma. Therefore, in addition to the typical SXR emission from electron excitation and recombination, the signals contained contributions from the x-ray emission due to charge exchange recombination (CXR). This was especially evident with the 0.3 μm Ti filter in place, as its transmission window from 150–450 eV covers the energy range, which passes the very bright carbon VI $n=2-1$, and $n=3-1$ CXR transitions. Specifically, the $n=2-1$ transition emits at 33.75 \AA (367 eV), and the $n=3-1$ transition emits at 28.48 \AA (435 eV), which corresponds to a transmission through the Ti filter of 50% and 61%, respectively. The quantitative effect that this CXR emission had on the overall SXR profile was assessed during discharge #133341 with neutral beam modulation. During this shot, one beam with a neutral beam injected power (P_{NBI}) of 2 MW (out a total P_{NBI} of 6 MW) changed from continuous operation to intermittent 5 ms “blips” spaced ~ 20 ms apart. The prompt CXR emission from these 2 MW P_{NBI} pulses contributed to $\sim 10\%$ of the total signal near the edge of the plasma down to a few percent toward the midradius as the natural beam attenuation reduced the CXR emission. Therefore, the total (6 MW P_{NBI}) CXR emission can comprise up to 30% of the total SXR intensity near the plasma edge when viewed with the 0.3 μm Ti filter. While this CXR emission can complicate quantitative modeling of the SXR plasma, it could also be of strong interest when considering, for example, beam-based diagnostics in the SXR wavelength range.

One dramatic advantage of the prototype compared to the previous multienergy SXR system is the high spatial resolution (~ 1.5 cm) and spatial oversampling. As a result, the prototype system was able to follow detailed changes in the SXR radial profile during 20 Hz edge-localized mode (ELM) cycles in high power NSTX H-mode discharges (Fig. 3). Previously, there have been indications in one or two channels of the lower resolution SXR diagnostics showing reductions in the edge plasma emission preceding an ELM event. However, with the higher spatial resolution of this prototype system, the SXR measurements show clearly a profile deg-

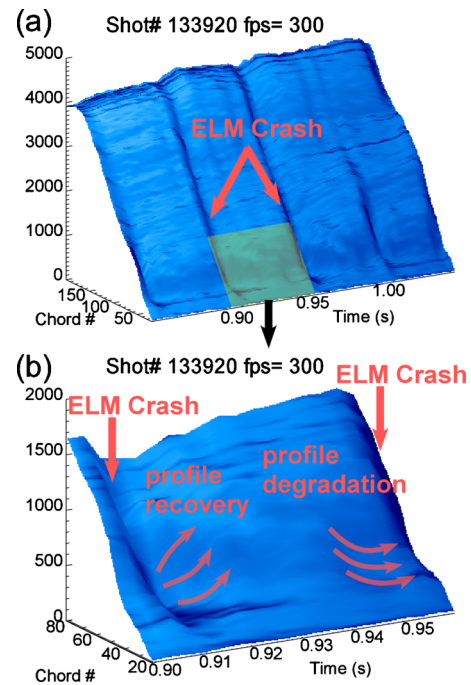


FIG. 3. (Color online) (a) The SXR intensity measurements from the edge to the core showing the effects of 20 Hz on the profile. (b) A magnified view of the outer ~ 15 cm of the SXR profile showing the details of the pre- and post-ELM profile dynamics.

radation encompassing the outer ~ 8 cm of the plasma edge ($R_{\text{tan}} \sim 137\text{--}145$ cm), 10–15 ms before the ELM crash, and then a subsequent profile recovery to “pre-ELM” levels before this cycle repeats. This observation highlights the utility and importance of continuous measurements with both high time (>1 kHz) and spatial resolution (~ 1 cm) to assist in the understanding of physical phenomena, especially at the plasma edge.

V. FINAL THOUGHTS

The single-energy prototype system based on an image intensified conversion of the SXR intensity profile to visible light is a relatively simple and compact diagnostic that provides good time (<10 kHz) and space (<1.5 cm) resolved measurements from the edge to the core of the plasma. The present system exceeds the SNR of the previous multienergy system by a factor of 2 and could be further optimized to offer an order of magnitude total improvement over the previous diagnostic system. Furthermore, the detailed spatial measurements provide the enticing capability to fully resolve the dynamics of edge profile evolution during interesting and important physical phenomena in NSTX plasmas.

Currently, the high image intensifier output brightness, required for imaging with the relatively low-sensitivity fast framing CMOS camera, forces operation in the MCP charge depletion regime, which nonlinearly reduces the gain in the channels with high intensity signals. However, one possible solution involves operating the MCP image intensifier at

lower intensity gain and adding a second stage image intensifier “diode” system, which forgoes the problematic MCP stage and uses only a photocathode coupled with a phosphor screen at high voltage.⁵ While the optical gain of such a device is low (40–50 W/W), it can provide the necessary high output brightness needed for the CMOS imaging system and allow the operation of the first stage MCP image intensifier in the lower output intensity, linear gain regime. The two-stage solution provides a viable path forward for an image intensifier-based ME-SXR diagnostic, which offers the potential of multiple filtered profiles combined with high spatial resolution without incurring the complication of a nonlinear, time-varying gain as observed with the prototype single stage MCP image intensifier.

ACKNOWLEDGMENTS

The authors appreciate and acknowledge the assistance from the NSTX support staff, machine operators, neutral beam operators, and the research team. This research is supported by DOE under Contract No. DE-AC02-09CH11466.

¹L. F. Delgado-Aparicio, D. Stutman, K. Tritz, M. Finkenthal, R. Bell, J. Hosea, R. Kaita, B. LeBlanc, L. Roquemore, and J. R. Wilson, *J. Appl. Phys.* **102**, 073304 (2007).

²L. F. Delgado-Aparicio, D. Stutman, K. Tritz, R. Vero, M. Finkenthal, G. Suliman, R. Kaita, R. Majeski, B. Stratton, L. Roquemore, and C. Tarrío, *Appl. Opt.* **46**, 6069 (2007).

³Vision Research, Inc., Phantom v4.2 data sheet, 2007, http://www.visionresearch.com/uploads/docs/Discontinued/V4/DS_v4x.pdf.

⁴J. L. Wiza, *Nucl. Instrum. Methods* **162**, 587 (1979).

⁵Proxitronic Detector Systems GmbH, Proxifier data sheet, http://www.proxitronic.de/datasheets/20091027_ebv.pdf.